FlatChem 37 (2023) 100469

Contents lists available at ScienceDirect

FlatChem

journal homepage: www.sciencedirect.com/journal/flatchem

Irida-graphene: A new 2D carbon allotrope

M.L. Pereira Júnior [a,*], W.F. da Cunha [b], W.F. Giozza [a], R.T. de Sousa Junior [a], L.A. Ribeiro Junior [b]

[a] Department of Electrical Engineering, Faculty of Technology, University of Brasília, Brasília, Brazil
[b] Institute of Physics, University of Brasília, Brasília, Brazil

ARTICLE INFO

Keywords:
New 2D carbon allotrope
Electronic structure
Mechanical and thermal properties
Density functional theory
Reactive molecular dynamics

ABSTRACT

Several 2D carbon-based materials have been computationally designed in the last years due to the success achieved by graphene. Using a bottom-up approach, we propose a new 2D all-sp^2 carbon allotrope, Irida-Graphene (IG). IG is composed of fused rings containing 3-6-8 carbon atoms. Density functional theory calculations and reactive (ReaxFF) molecular dynamics simulations were carried out to examine its mechanical, structural, electronic, and optical properties. DFT results showed that IG exhibits good dynamical and thermal stabilities. Its estimated elastic modulus is approximately 396 GPa. IG is a metallic non-magnetic material, and presents a Dirac cone above the Fermi level in the center of the band. The intense optical activity of IG is restricted to the infrared and violet regions. IG can act as a violet collector for photon energies of about 3.0 eV since it presents very low reflectivity and refractive index greater than one.

1. Introduction

The design [1,2] and synthesis [3–5] of new carbon allotropes have experienced enormous growth since the advent of graphene [6,7]. Its 2D honeycomb arrangement with an atomic thickness exhibits unique mechanical, optical, and electronic properties, which are of significant interest for many potential applications in nanoelectronics [8]. Due to this reason, several 2D carbon-based materials have been computationally proposed in the last few years [9–17]. The monolayer amorphous carbon [3], biphenylene network [4], and monolayer fullerene network [5] were synthesized recently. The successful synthesis of these materials has helped to stimulate the designing of new 2D carbon allotropes that can be obtained experimentally.

A trend in developing new carbon allotropes has been to propose structures with non-hexagonal rings and large pores. The ultimate motivation is that carbon-based materials with non-hexagonal ring structures are better adsorbers of Lithium atoms when contrasted with graphene [18,19]. One can highlight the popgraphene (composed of 5–8-5 carbon rings) [16], phagraphene [14], and psi-graphene [20], which are composed of 5–6-7 carbon rings. They are intrinsically metallic and have a high theoretical capacity to adsorb Li atoms (1487, 556, and 372 mA h g^{-1}, respectively), which are crucial traits for developing efficient Li-ion batteries. Based on these performances for Li storage capacity, it can be helpful in energy storage applications to design other porous 2D metallic materials containing fused rings with eight carbon atoms.

In this study, we employed a bottom-up approach to computationally propose a new 2D all-sp^2 carbon allotrope composed of 3–6-8 rings named Irida-Graphene (IG). This name is due to its atomic arrangement that resembles the flower (*Sisyrinchium Halophilum - Iridaceae*), popularly called "Nevada Blue-Eyed Grass" in the United States (see Fig. 1). We carried out density functional theory (DFT) and reactive (ReaxFF) molecular dynamics (MD) simulations to study the electronic, optical, and mechanical properties of this material. DFT and MD results revealed that IG is metallic and structurally stable, as confirmed by its integrity at 4176 K and by the absence of imaginary phonon modes in its phonon dispersion spectra. Its optical activity is restricted to the infrared and violet regions. All the MD results are presented in the Supplementary Material.

2. Methodology

The lattice structure of IG is shown in Fig. 1. Its unit cell is flat and composed of 12 carbon atoms. As one can see in this figure, IG is a 2D all-sp^2 carbon allotrope composed of fused 3-6-8 rings. Its structure has three types of carbon–carbon bonds: C_1-C_2/C_{11}-C_{12}/C_1-C_5/C_2-C_8/C_8-C_{11} = 1.439 Å, C_2-C_3/C_4-C_5/C_1-C_6/C_7-C_{12}/C_8-C_9/C_{10}-C_{11} = 1.410 Å, and C_3-C_4/C_3-C_7/C_4-C_7/C_6-C_{10}/C_9-C_{10} = 1.413 Å. IG crystallizes in the

* Corresponding author.
E-mail address: marcelo.lopes@unb.br (M.L. Pereira Júnior).

https://doi.org/10.1016/j.flatc.2023.100469
Received 22 August 2022; Received in revised form 13 December 2022; Accepted 2 January 2023
Available online 4 January 2023

hexagonal P6/mmm (191) space group. Its formation energy is −6.96 eV/atom. The areal density of carbon atoms in IG is $3.45 \times 10^{15}\text{cm}^{-2}$. This value is similar to the graphene one ($3.82 \times 10^{15}\text{cm}^{-2}$) [21].

All first-principles calculations were based on DFT theory as implemented in the SIESTA code [22–24]. These calculations were carried out within the scope of the generalized gradient approximation (GGA) with the Perdew-Burke-Ernzerhof (PBE) [25,26] functional for the exchange–correlation term. Norm-conserving Troullier-Martins pseudopotential [27] was employed to describe the core electrons. The wave functions were defined by localized atomic orbitals and a double-zeta plus polarization (DZP) basis set.

We used 500 Ry for kinetic energy cut-off, sampling the reciprocal space with 30 × 30 × 1 k-point grid. The vacuum region along the z-direction is set to 10 $\mathring{A}$ to prevent spurious interactions between the sheet and its periodic images. The basis vector along the z-direction was fixed during the lattice optimization. The other vectors and atoms were fully relaxed. The convergence criterion for maximum forces on each atom was 0.001 eV/$\mathring{A}$. To investigate the stability of IG, we performed phonon dispersion calculations based on the force constant algorithm for $T = 0$ K, as implemented in Phonopy [28], and Born–Oppenheimer *ab initio* molecular dynamics simulations (AIMD) for 300 K, 500 K, and 1000 K with the canonical ensemble NVT. For the electronic band structure calculation, we considered the following path along the lattice: $\Gamma = (0,0)$ to $K = (0,1/2)$ to $Y = (1/3,1/3)$ to $Z = (1/2,0)$ to $\Gamma = (0,0)$.

An external electric field of value 1.0 V/$\mathring{A}$ was applied along three possible polarization planes to estimate the optical coefficients. The optical coefficients were come from complex dielectric function $\epsilon = \epsilon_1 + i\epsilon_2$, in which the imaginary part, ϵ_2, is derived from the direct interband transitions through Fermi's golden rule. A detailed description of the procedure to calculate the optical properties (used in this work) is given in reference [29].

3. Results

The discussion is divided into three subsections: I) structural stability and mechanical properties and II) electronic and optical properties. The Supplementary Material presents the MD snapshots for the uniaxial tensile loading and the heating of IG, MD stress–strain curves, and the Density of States (DOS) for calculations, which included spin polarization. We also show the real and imaginary parts of the dielectric constant as a function of photon energy for IG. The crystallographic information file (CIF) containing the IG structure is also included in the Supplementary Material.

3.1. Structural stability and mechanical properties

We examined the dynamical stability of IG by calculating the phonon dispersion relations along the high symmetry directions shown in Fig. 2.

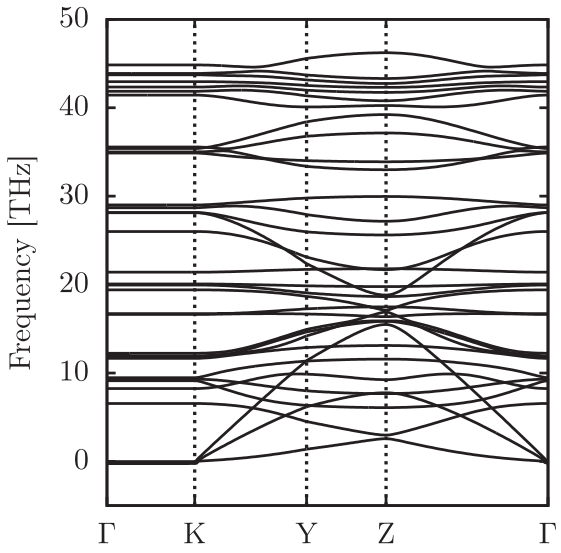

Fig. 2. Phonon band structure of Irida-Graphene with a 4 × 4 × 1 supercell.

Furthermore, we carried out 20 ps of AIMD at 300 K, 500 K, and 1000 K to ensure the IG stability, as depicted in Fig. 3. The 300 K and 500 K cases are shown in the Supplementary Material. In Fig. 2, one can see that most phonon frequencies are positive without any imaginary modes in the Brillouin zone. Imaginary frequencies (softened modes) appear in the spectrum but are less than 0.5% of the total frequencies. Physically, intrinsic ripples of 2D carbon-based materials can yield negative phonon modes due to significant out-of-plane atomic fluctuations. This feature is also present in graphene [30–32]. In this sense, the phonon spectrum confirms the IG dynamical and structural stability. Moreover, the highest phonon frequency is about 47 THz, similar to graphene [33] and indicating the presence of only sp^2 carbon–carbon bonds.

Fig. 3 shows the results for the AIMD simulation at 1000 K. The insets illustrate the top and side views for the AIMD snapshot of the IG lattice in the final stage of the simulation. For this case, we adopted a 2 × 2 × 1 supercell containing 64 carbon atoms. One can note that the total energy per atom for the IG lattice fluctuates around a steady level in the heating process (equilibrium state). Moreover, in the MD snapshot for IG at 20 ps, the lattice structure maintains its planarity and has no bond reconstructions. The features revealed in the AIMD simulations suggest that IG has good thermal stability. It is worth stressing that other approaches have been successfully employed to study the stability of nanostructured materials. Machine-learning interatomic potentials were developed to evaluate their phononic properties, lattice thermal conductivity, and piezoelectric/flexoelectric responses [34,35].

The mechanical properties of IG are also studied through DFT sim-

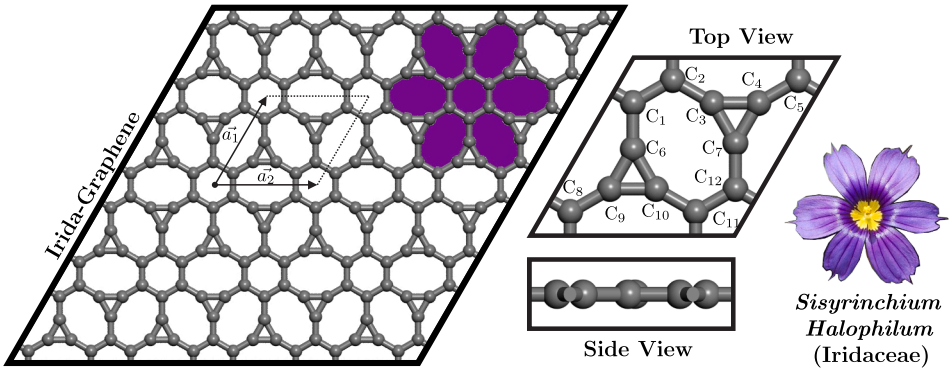

Fig. 1. Schematic representation of the Irida-Graphene structure. The right panels show the top and side views of its unit cell and a representation of the Sisyrinchium Halophilum - Iridaceae flower. The lattice vectors are $a_1 = a_2 = 6.34$ $\mathring{A}$.

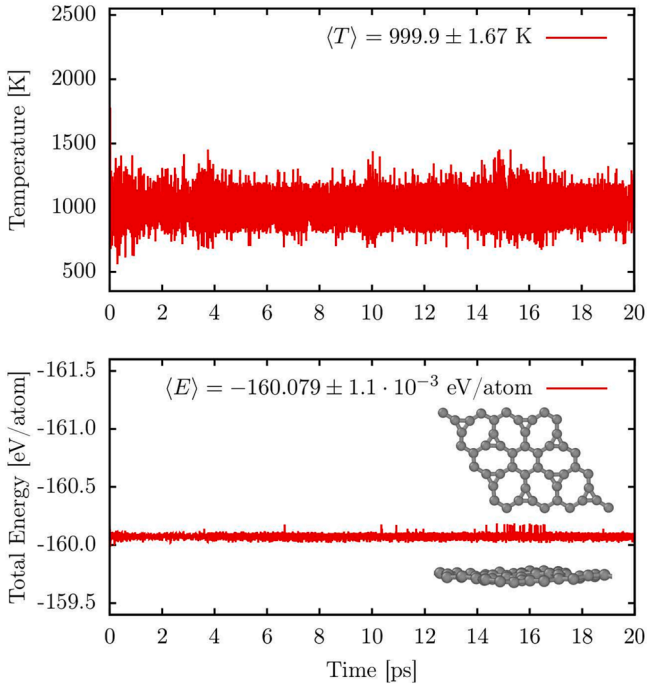

Fig. 3. Time evolution of the total energy per atom in the IG lattice at 1000 K. The insets show the top and side views of the final AIMD snapshot at 20 ps.

ulations. As a general trend, IG lattices have two well-defined stages for the stress–strain relationship. The IG lattice has periodic boundary conditions and is subjected to a uniaxial tensile strain between 0–30%. Fig. 4 presents the stress–strain curve under uniaxial strain loading along the *x* and *y* directions (blue and red circles, respectively). This figure shows the stress–strain interplay until the moment of the lattice fracture. The Young's modulus values YM_X and YM_Y (along the x- and y-directions, respectively) are calculated considering the first linear regime, up to 5% of strain for each curve.

In the first regime, the stress rises sharply up to 10% of strain in both directions. The IG lattice keeps its integrity, but the carbon rings suffer deformations during the stretching process. Between 10%–18% and 10%–19% of strain in the x- and y-direction, respectively, the IG lattice suffers its first bond breaking, producing a crack, which propagates through the structure. Above these critical strain thresholds (second regime for the stress–strain relationship), the stress drops abruptly, indicating the rupture of the IG lattice.

The estimated elastic moduli are $YM_X = 396$ GPa and $YM_Y = 397$ GPa. These results revealed that IG has piratically isotropic mechanical properties, as expected from the structure topology. The eight-membered rings of carbon atoms are responsible for the smaller mechanical resilience presented by IG compared with graphene (about 1 TPa) [36]. However, the *YM* values calculated for IG are similar to those reported for other graphene-like allotropes [37,38]. The IG fracture strain (*FS*) and ultimate stress (*US*) are $FS = 18\%$ and $US = 46.8$ GPa in the x-direction and $FS = 19.0\%$ and $US = 52.9$ GPa in the y-direction. It is worth mentioning that *FS* is obtained from the strain percentage corresponding to the higher stress value, i.e., the *US*. These mechanical properties are also similar to those for other graphene-like allotropes [37,38].

3.2. Electronic and optical properties

The calculated band structure, related density of states (DOS), and partial density of states (PDOS) are shown in Fig. 5. The inset in Fig. 5(a) illustrates the high symmetry directions used to calculate the electronic band structure. On the GGA/PBE level, no band gap was found between the valence and conduction bands (see Fig. 5), indicating that IG is metallic. The DOS near the Fermi level is essentially formed by $2p_z$ atomic orbitals, confirming its metallic signature. We performed calculations, including spin polarization. The DOS results show that the material is not magnetic (see Supplementary Material).

IG valence bands are predominantly composed of $2p_z$ atomic orbitals, with a small contribution of $2p_y$ orbitals. On the other hand, the conduction bands are formed by 2s, $2p_y$, and $2p_z$ orbitals with higher contributions. This trend for the higher contribution of $2p_z$ orbitals to the conduction bands is typical in 2D carbon-based systems [39]. A Dirac cone is situated above the Fermi level and in the center of the band

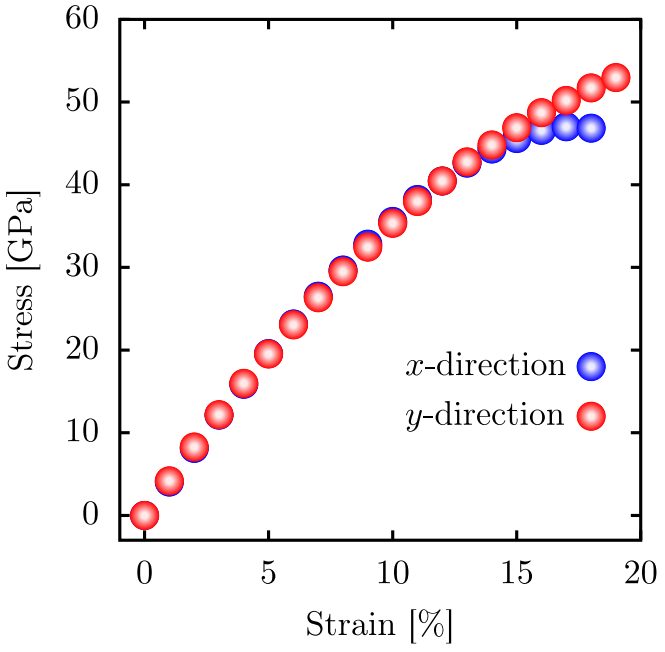

Fig. 4. Stress–strain relationships of IG under uniaxial tensile loading in (blue) the x-direction and (red) y-direction.

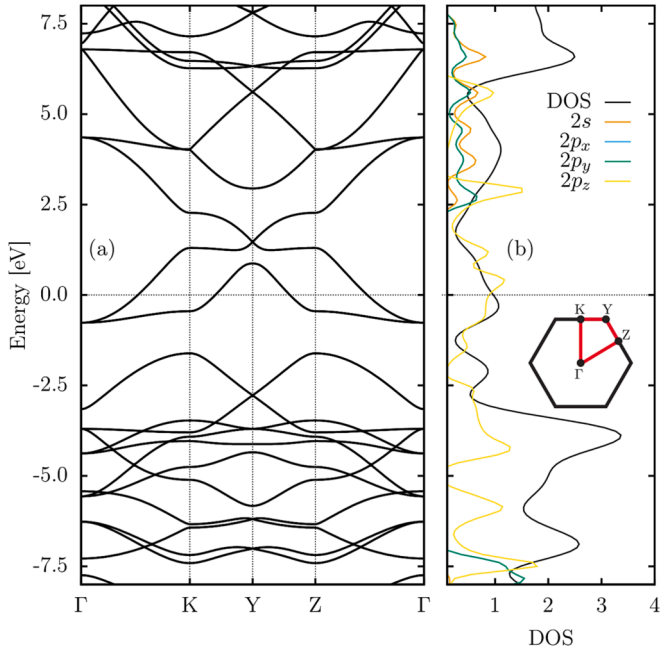

Fig. 5. Electronic band structure and related partial density of states (PDOS) of IG. We considered the following path along the high symmetry directions: $\Gamma = (0,0)$ to $K = (0,1/2)$ to $Y = (1/3,1/3)$ to $Z = (1/2,0)$ to $\Gamma = (0,0)$.

at the *Y*-point. Other 2D materials also present such a trend for the localization of the Dirac cone [10,14].

Finally, we discuss the optical properties of IG. Figs. 6(a–c) show the absorption coefficient (α), refractive (η), and reflectivity (R) indexes as a function of the photon energy value for the light propagation in the x-direction. The real and imaginary parts of the dielectric constant as a function of photon energy for IG are shown in the Supplementary Material. Importantly, we did not notice a significant difference in the optical activity of the IG between the x- and y-directions. In this figure, one can note that the intense optical activity of IG is restricted to the infrared and violet regions, and a small activity in the ultra-violet region can also be noted.

The α profile presented in Fig. 6(a) revealed that the first optical transition peak occurs for nearly the same photon energy in all directions, about 1.0 eV (i.e., within the infrared spectrum). The second peak transition peak occurs within the violet region, about 3.0 eV. The maximum absorption intensities are approximately 2.0×10^5 cm^{-1} and 1.2×10^5 cm^{-1} within the infrared and violet regions, respectively. In the context of carbon-based materials, intense absorption within the infrared region denotes the presence of sp^2-like carbons [40].

Figs. 6(b) and 6(c) show the refractive and reflectivity indexes, respectively, as a function of the photon energy. The maximum peak for refractive index occurs at 0.7 eV, as depicted in Fig. 6(b). Light attenuation occurs for photon energies higher than 0.7 eV. η values converge to 1.2, suggesting that the incident light tends to be refracted similarly in all directions.

The reflective index has the maximum peak at 1.2 eV and drops to almost zero in the infrared region. A small reflection activity of IG, around 5%, is noted within the violet region. In this sense, all the incident violet and ultra-violet lights tend to be absorbed, as shown in Fig. 6(c). On the other hand, almost 50% of the incident light is reflected in the infrared region. These results suggest that IG can act as a violet collector for photon energies of about 3.0 eV since it presents very low reflectivity and refractive index greater than one.

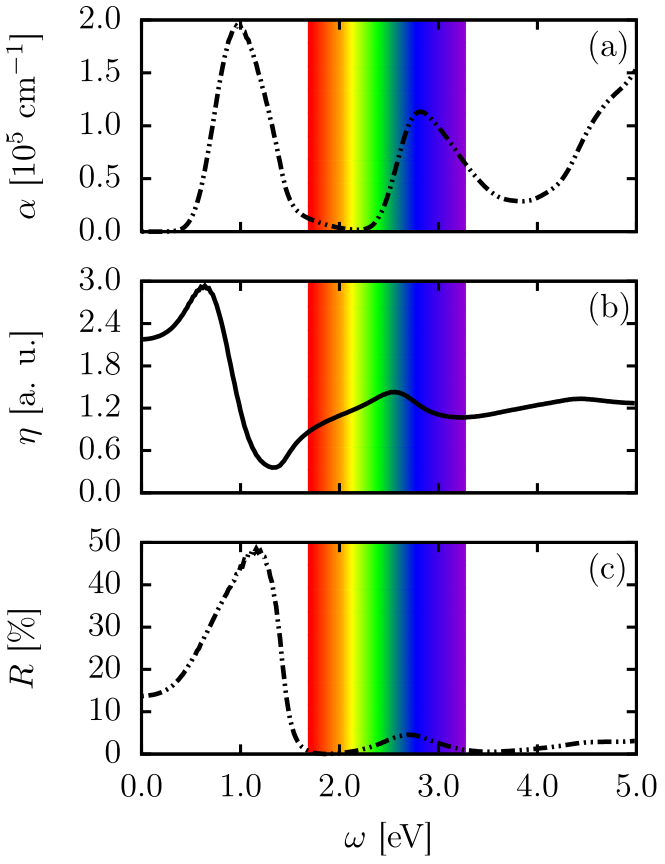

Fig. 6. Irida-graphene absorption coefficient (α), refractive (η), and reflectivity (R) indexes as a function of the photon energy.

4. Conclusions

In summary, we used DFT and reactive ReaxFF MD simulations to propose a new 2D all-sp^2 carbon allotrope named Irida-Graphene (IG) by employing a bottom-up approach. IG is composed of fused rings containing 3–6-8 carbon atoms. To examine the structural stability of IG, we calculated its phonon spectrum and formation energy. We found that the IG formation energy is −6.96 eV/atom. AIMD simulations were also used to confirm its structural and dynamic stability.

The calculated phonon frequencies confirm the stability of IG. Moreover, the highest phonon frequency is about 47 THz, similar to graphene and indicating the presence of only sp^2 carbon–carbon bonds. In the AIMD simulations, the total energy per atom for the IG lattice fluctuates around a steady level during the heating process at 1000 K and 20 ps. The lattice structure maintained its planarity with no bond reconstructions at the final stage of the simulation. These features suggest that IG also has good thermal stability.

The estimated elastic moduli are $YM_X = 396$ GPa and $YM_Y = 397$ GPa. IG has apparent in-plane isotropic mechanical properties, as expected from its topology. The eight-membered rings of carbon atoms are responsible for the smaller mechanical resilience presented by IG compared with graphene (about 1 TPa).

In the calculated band structure, no band gap was found between the valence and conduction bands, indicating that IG is metallic. A Dirac cone is situated above the Fermi level and in the center of the band at the *Y*-point. The DOS near the Fermi level is essentially formed by 2p$_z$ atomic orbitals, confirming its non-magnetic metallic signature.

The intense optical activity of IG is restricted to the infrared and violet regions. A small optical activity in the ultra-violet zone was also noted. In carbon-based materials, intense infrared absorption denotes the presence of sp^2-like carbons. A small reflection activity of IG (around 5%) is noted in the violet zone. All the incident violet and ultra-violet lights tend to be absorbed.

On the other hand, almost 50% of the incident light is reflected in the infrared region. These results suggest that IG can act as a violet collector for photon energies of about 3.0 eV since it presents very low reflectivity and refractive index greater than one.

Regarding possible applications of IG in flexible electronics, its unique topology, and structural and thermal stabilities suggest that, if synthesized, this material (or other nanostructured material with similar topology) can act for developing, for example, efficient Li-ion batteries.

CRediT authorship contribution statement

M.L. Pereira Júnior: Conceptualization, Methodology, Software, Validation, Formal analysis, Investigation, Resources, Data curation, Writing - original draft, Writing - review & editing, Visualization, Supervision, Project administration. **W.F. da Cunha:** Validation, Formal analysis, Investigation, Resources, Data curation, Writing - original draft. **W.F. Giozza:** Validation, Formal analysis, Investigation, Resources, Data curation, Writing - original draft, Writing - review & editing, Funding acquisition. **R.T. de Sousa Junior:** Writing - review & editing, Visualization, Supervision, Project administration, Funding acquisition. **L.A. Ribeiro Junior:** Conceptualization, Methodology, Validation, Formal analysis, Investigation, Resources, Data curation, Writing - original draft, Writing - review & editing, Visualization, Supervision, Project administration, Funding acquisition.

Declaration of Competing Interest

The authors declare that they have no known competing financial interests or personal relationships that could have appeared to influence

the work reported in this paper.

Data availability

The research data/code are described in the paper's methodology.

Acknowledgements

The authors gratefully acknowledge the financial support from Brazilian research agencies CNPq and FAP-DF. L.A.R.J acknowledges the financial support from a Brazilian Research Council FAP-DF grants 00193 −00000853/2021 −28, 00193.00001808/2022-71, and 00193-00001247/2021-20 and CNPq grants 302236/2018 −0 and 350176/2022 −1, respectively. M.L.P.J and L.A.R.J acknowledges CENAPAD-SP for providing the computational facilities. W.F.C and W.F.G acknowledge the financial support from FAPDF grants 00193 −00000857/2021 −14 and 00193 −00000811/2021 −97, respectively. R.T.S.J. gratefully acknowledges CNPq (Grants 312180/2019-5 PQ-2 and 465741/2014-2 INCT on Cybersecurity). R.T.S.J. and L.A.R.J. gratefully acknowledge the support from ABIN grant 08/2019. M.L.P. J. and L.A.R.J. acknowledge Núcleo de Computação de Alto Desempenho (NACAD) for providing the computational facilities through the Lobo Carneiro supercomputer. M.L.P. J. and L.A.R.J. acknowledge the National Laboratory for Scientific Computing (LNCC/MCTI, Brazil) for providing HPC resources of the SDumont supercomputer, which have contributed to the research results reported within this paper. URL: http://sdumont.lncc.br. L.A.R.J. thanks Fundação de Apoio à Pesquisa (FUNAPE), Edital 02/2022 – Formulário de Inscrição N.4, for the financial support.

Appendix A. Supplementary data

Supplementary data associated with this article can be found, in the online version, athttps://doi.org/10.1016/j.flatc.2023.100469.

References

[1] L. Yang, H.Y. He, B.C. Pan, Theoretical prediction of new carbon allotropes, J. Chem. Phys. 138 (2) (2013), 024502.
[2] Run-Sen Zhang, Jin-Wu Jiang, The art of designing carbon allotropes, Front. Phys. 14 (1) (2019) 1–17.
[3] Chee-Tat Toh, Hongji Zhang, Junhao Lin, Alexander S Mayorov, Yun-Peng Wang, Carlo M Orofeo, Darim Badur Ferry, Henrik Andersen, Nurbek Kakenov, Zenglong Guo, et al., Synthesis and properties of free-standing monolayer amorphous carbon, Nature 577 (7789) (2020) 199–203.
[4] Qitang Fan, Linghao Yan, Matthias W Tripp, Ondřej Krejčí, Stavrina Dimosthenous, Stefan R Kachel, Mengyi Chen, Adam S Foster, Ulrich Koert, Peter Liljeroth, et al., Biphenylene network: A nonbenzenoid carbon allotrope, Science 372 (6544) (2021) 852–856.
[5] Lingxiang Hou, Xueping Cui, Bo Guan, Shaozhi Wang, Ruian Li, Yunqi Liu, Daoben Zhu, Jian Zheng, Synthesis of a monolayer fullerene network, Nature 606 (7914) (2022) 507–510.
[6] Andre Konstantin Geim, Graphene: status and prospects, Science 324 (5934) (2009) 1530–1534.
[7] Andre K Geim, Konstantin S Novoselov, The rise of graphene. In Nanoscience and technology: a collection of reviews from nature journals</hi>, World Scientific, 2010, pp. 11–19.
[8] R.M. Westervelt, Graphene nanoelectronics, Science 320 (5874) (2008) 324–325.
[9] Andrey N. Enyashin, Alexander L. Ivanovskii, Graphene allotropes. Physica Status Solidi (b), 248(8):1879–1883, 2011.
[10] Xu. Li-Chun, Ru-Zhi Wang, Mao-Sheng Miao, Xiao-Lin Wei, Yuan-Ping Chen, Hui Yan, Woon-Ming Lau, Li-Min Liu, Yan-Ming Ma, Two dimensional dirac carbon allotropes from graphene, Nanoscale 6 (2) (2014) 1113–1118.
[11] Humberto Terrones, E. Mauricio Terrones, N Grobert Hernández, Jean-Christophe Charlier, P.M. Ajayan, New metallic allotropes of planar and tubular carbon, Phys. Rev. Lett. 84 (8) (2000) 1716.
[12] Maria Lúcia Álvares Paz, Aldilene Saraiva-Souza, Vincent Meunier, and Eduardo Costa Gir ao. Naphthylenes: 1d and 2d carbon allotropes based on naphthyl units. Carbon, 153:792–803, 2019.
[13] Lu. Haigang, Si-Dian Li, Two-dimensional carbon allotropes from graphene to graphyne, J. Mater. Chem. C 1 (23) (2013) 3677–3680.
[14] Zhenhai Wang, Xiang-Feng Zhou, Xiaoming Zhang, Qiang Zhu, Huafeng Dong, Mingwen Zhao, Artem R Oganov, Phagraphene: a low-energy graphene allotrope composed of 5–6–7 carbon rings with distorted dirac cones, Nano Lett. 15 (9) (2015) 6182–6186.
[15] Shunhong Zhang, Jian Zhou, Qian Wang, Xiaoshuang Chen, Yoshiyuki Kawazoe, Puru Jena, Penta-graphene: A new carbon allotrope, Proc. Nat. Acad. Sci. 112 (8) (2015) 2372–2377.
[16] Shuaiwei Wang, Baocheng Yang, Houyang Chen, Eli Ruckenstein, Popgraphene: a new 2d planar carbon allotrope composed of 5–8–5 carbon rings for high-performance lithium-ion battery anodes from bottom-up programming, J. Mater. Chem. A 6 (16) (2018) 6815–6821.
[17] Susmita Jana, Arka Bandyopadhyay, Sujoy Datta, Debaprem Bhattacharya, Jana Debnarayan, Emerging properties of carbon based 2d material beyond graphene, J. Phys.: Condens. Matter (2021).
[18] Yu. Yang-Xin, Graphenylene: a promising anode material for lithium-ion batteries with high mobility and storage, J. Mater. Chem. A 1 (43) (2013) 13559–13566.
[19] Jaewook Kim, Sungwoo Kang, Jaechang Lim, Woo Youn Kim, Study of li adsorption on graphdiyne using hybrid dft calculations, ACS Appl. Mater. Interfaces 11 (3) (2018) 2677–2683.
[20] Xiaoyin Li, Qian Wang, Puru Jena, ψ-graphene: a new metallic allotrope of planar carbon with potential applications as anode materials for lithium-ion batteries, J. Phys. Chem. Lett. 8 (14) (2017) 3234–3241.
[21] Eric Pop, Vikas Varshney, Ajit K Roy, Thermal properties of graphene: Fundamentals and applications, MRS Bull. 37 (12) (2012) 1273–1281.
[22] José M Soler, Emilio Artacho, Julian D Gale, Alberto García, Javier Junquera, Pablo Ordejón, Daniel Sánchez-Portal, The siesta method for ab initio order-n materials simulation, J. Phys.: Condens. Matter 14 (11) (2002) 2745.
[23] Emilio Artacho, Eduardo Anglada, Oswaldo Diéguez, Julian D Gale, Alberto García, Javier Junquera, Richard M Martin, Pablo Ordejón, José Miguel Pruneda, Daniel Sánchez-Portal, et al., The siesta method; developments and applicability, J. Phys.: Condens. Matter 20 (6) (2008), 064208.
[24] Emilio Artacho, Daniel Sánchez-Portal, Pablo Ordejón, Alberto Garcia, José M Soler, Linear-scaling ab-initio calculations for large and complex systems, Physica Status Solidi (b) 215 (1) (1999) 809–817.
[25] John P Perdew, Kieron Burke, Matthias Ernzerhof, Generalized gradient approximation made simple, Phys. Rev. Lett. 77 (18) (1996) 3865.
[26] Matthias Ernzerhof, Gustavo E Scuseria, Assessment of the perdew–burke–ernzerhof exchange-correlation functional, J. Chem. Phys. 110 (11) (1999) 5029–5036.
[27] Norman Troullier, José Luís Martins, Efficient pseudopotentials for plane-wave calculations, Phys. Rev. B 43 (3) (1991) 1993.
[28] Atsushi Togo, Isao Tanaka, First principles phonon calculations in materials science, Scripta Mater. 108 (2015) 1–5.
[29] Raphael M Tromer, Levi C Felix, Luiz A Ribeiro, Douglas S Galvao, Optoelectronic properties of amorphous carbon-based nanotube and nanoscroll, Physica E Low-dimensional Systems and Nanostructures 130 (2021), 114683.
[30] Seungjun Lee, Effect of intrinsic ripples on elasticity of the graphene monolayer, Nanoscale Res. Lett. 10 (1) (2015) 1–9.
[31] Annalisa Fasolino, JH Los, and Mikhail I Katsnelson. Intrinsic ripples in graphene. Nature Mater., 6(11):858–861, 2007.
[32] Hu. Yangfan, Jiapeng Chen, Biao Wang, On the intrinsic ripples and negative thermal expansion of graphene, Carbon 95 (2015) 239–249.
[33] Houfu Song, Jiaman Liu, Bilu Liu, Wu. Junqiao, Hui-Ming Cheng, Feiyu Kang, Two-dimensional materials for thermal management applications, Joule 2 (3) (2018) 442–463.
[34] T. Rabczuk, X. Zhuang, B. Mortazavi, B. Javvaji, F. Shojaei, A.V. Shapeev, Exceptional piezoelectricity, high thermal conductivity and stiffness and promising photocatalysis in two-dimensional mosi 2 n 4 family confirmed by first-principles, Nano Energy 82 (2021), 105716–105716.
[35] Bohayra Mortazavi, Evgeny V Podryabinkin, Ivan S Novikov, Timon Rabczuk, Xiaoying Zhuang, Alexander V Shapeev, Accelerating first-principles estimation of thermal conductivity by machine-learning interatomic potentials: A mtp/shengbte solution, Comput. Phys. Commun. 258 (2021), 107583.
[36] Changgu Lee, Xiaoding Wei, Jeffrey W Kysar, James Hone, Measurement of the elastic properties and intrinsic strength of monolayer graphene, Science 321 (5887) (2008) 385–388.
[37] Chao Sui, Yushun Zhao, Zhisen Zhang, Jianying He, Zhiliang Zhang, Xiaodong He, Chao Wang, Wu. Jianyang, Morphology-controlled tensile mechanical characteristics in graphene allotropes, ACS Omega 2 (7) (2017) 3977–3988.
[38] Hao Sun, Sankha Mukherjee, Matthew Daly, Ajay Krishnan, Manohar Harsha Karigerasi, Chandra Veer Singh, New insights into the structure-nonlinear mechanical property relations for graphene allotropes, Carbon 110 (2016) 443–457.
[39] Gui Gui, Jin Li, Jianxin Zhong, Band structure engineering of graphene by strain: First-principles calculations, Phys. Rev. B 78 (7) (2008), 075435.
[40] S.E. Rodil, Infrared spectra of amorphous carbon based materials, Diamond and related materials 14 (8) (2005) 1262–1269.